

# Parameter selection for model updating with global sensitivity analysis.

Zhaoxu Yuan<sup>a</sup>, Peng Liang<sup>b</sup>, Tiago Silva<sup>c</sup>, Kaiping Yu<sup>a,\*</sup>  
and John E Mottershead<sup>b,\*</sup>

<sup>a</sup>*Harbin Institute of Technology (HIT), Department of Astronautical Science and Mechanics, P.O. Box 304, No.92 West Dazhi Street, Harbin 150001, Peoples' Republic of China.*

<sup>b</sup>*University of Liverpool, Department of Mechanical, Materials and Aerospace Engineering, The Quadrangle, Liverpool L69 3GH, United Kingdom.*

<sup>c</sup>*Universidade Nova de Lisboa, UNIDEMI, Department of Mechanical and Industrial Engineering, Campus da Caparica, 2829-516 Caparica, Portugal.*

\*Corresponding authors

John Mottershead: j.e.mottershead @liverpool.ac.uk

Kaiping Yu: yukp@hit.edu.cn

## Abstract

The problem of selecting parameters for stochastic model updating is one that has been studied for decades, yet no method exists that guarantees the 'correct' choice. In this paper, a method is formulated based on global sensitivity analysis using a new evaluation function and a composite sensitivity index that discriminates explicitly between sets of parameters with correctly-modelled and erroneous statistics. The method is applied successfully to simulated data for a pin-jointed truss structure model in two studies, for the cases of independent and correlated parameters respectively. Finally, experimental validation of the method is carried out on a frame structure with uncertainty in the position of two masses. The statistics of mass positions are confirmed by the proposed method to be correctly modelled using a Kriging surrogate.

**Keywords:** Model updating, parameter selection, uncertainty, global sensitivity.

## 1 Introduction

Finite element model updating has become a useful and widely-used tool to improve the correlation between test data and computational prediction [1], [2]. Usually, there are many candidate parameters that could be used to produce the required change in the model output. One approach is to allow all the parameters to participate in the updating procedure, but to constrain them in the sense of the minimum norm. An alternative approach is to select a certain subset of the updating parameters based on physical meaning or engineering experience [3] – this introduces the problem of parameter selection for model updating.

In the early days, parameter selection was done by using engineering experience, but is considered to be too subjective. Ahmadian et al. [4] used a matrix decomposition to update the eigenvalues and eigenvectors of individual finite elements or substructures. This approach often leads to non-physical updated models that reproduce test data with good accuracy. Of course, the need (or otherwise) for physical meaning depends upon the purpose of the model. Most parameter selection methods are based upon the matrix of local sensitivities, normally evaluated through gradients or partial derivatives of the response of model at the updating parameters.

There are numerous studies based on local sensitivity methods [5], [6]. Subset parameter selection methods choose parameters or groups of parameters that minimize a residual function for updating [7], [8], [9]. Friswell et al. [3] developed an improved parameter subset selection method by taking account of side constraints on the parameter values. Kim and Park [10][11] presented an improved parameter selection method by creating substructures from elements with similar sensitivity. The problem with local sensitivity methods is that they are based entirely upon the local gradient of the response of an analytical model (at a certain parameter point), which means that such methods are only applicable in the space close to the initial parameter estimate. Also, they are only able to identify ‘sensitive’ parameters and cannot locate the uncertainty in the model because local sensitivity methods take no account of test data. Global sensitivity methods, as the name implies, offer advantages not possessed by local methods.

There are several statistics-based parameter selection approaches, such as the Bayesian evidence statistic [12] and the F-test [13], [14]. Among these methods, global sensitivity analysis (GSA) [15] is the most widely used. In contrast to local sensitivity analysis, such methods consider the whole variation range of the inputs [16] and are therefore referred to as 'global'. The calculation of GSA indices may be carried out in different ways. For example, Boscato et al. [17] used a derivative-based approach, also known as the elementary effects (EE) method. They concluded that GSA is better suited than local sensitivity-based methods to complex structures, such as historical buildings with high uncertainty. Wan and Ren [18] used the more widely accepted variance-based GSA method using Sobol indices to give a more sophisticated measurement of the input effect on the output. This was done by calculating the indices by integration over the whole input domain rather than a limited selection of observations.

Wan and Ren [18], used the sum of squares of modal frequency residuals normalized by the standard deviation as the objective function and a Gaussian process emulator (GPE) to replace the expensive finite element code. They concluded that the total sensitivity indices should be used along with the first-order sensitivity indices to avoid discarding the parameters with the negligible first-order effects but significant total sensitivity. Sudret [19] described an improved method whereby the Sobol indices were determined analytically from the generalized polynomial chaos expansion (PCE). Thus, the computational cost of the sensitivity indices was practically reduced to that of estimating the PCE coefficients. Practical application of GSA research in damage identification includes the full-scale seven-storey shear wall building structure tested on the UCSD-NEES shake table [20].

Silva et al. [21] developed a decomposition of the scaled output covariance matrix using the columns of the local sensitivity matrix. They selected the parameters that contributed most to the test output covariances by projecting the sensitivity-matrix columns onto the matrix of left singular vectors (with non-zero singular values). This has the advantage of computational efficiency; not requiring the expensive sampling required for the computation of Sobol indices, but is not able to discriminate between parameter uncertainty that is accurately modelled and that which is not. It is only the latter that accounts for the difference in output

variability between the test and the model. This latter point (on the discrimination between true and erroneous parameter distributions) also applies to methods based on objective functions that take the form of the square of the response residuals normalised by the mean or standard deviation – they aim only to find the parameters that reproduce the output variability and not necessarily the erroneous parameters.

The purpose of this research is to propose a global sensitivity-based parameter selection method, based on an evaluation function, with built-in test data, and based on the multivariate normal distribution. Then by using the global sensitivity method, a composite sensitivity index is formed, which separates sets of parameters with correctly-modelled and erroneous statistics. This represents a more powerful parameter selection approach than is presently available by existing methods, which only select parameters that contribute to observed variability (whether or not the statistics of the parameters are modelled correctly). The effectiveness and robustness are validated with several computational cases on a truss model. Both the cases of independent parameters and correlated parameters are studied and discussed. After the simulation cases, an experimental frame with uncertain mass locations is studied. The positions of masses on the structure are arranged on the basis of a correlated number pair array. The goal, in this case, is to correctly identify that the uncertain mass positions are responsible for observed natural frequency variation.

## **2 Parameter selection by GSA**

The parameter selection method is described by the flowchart shown in Figure 1 and details are provided in the following sections.

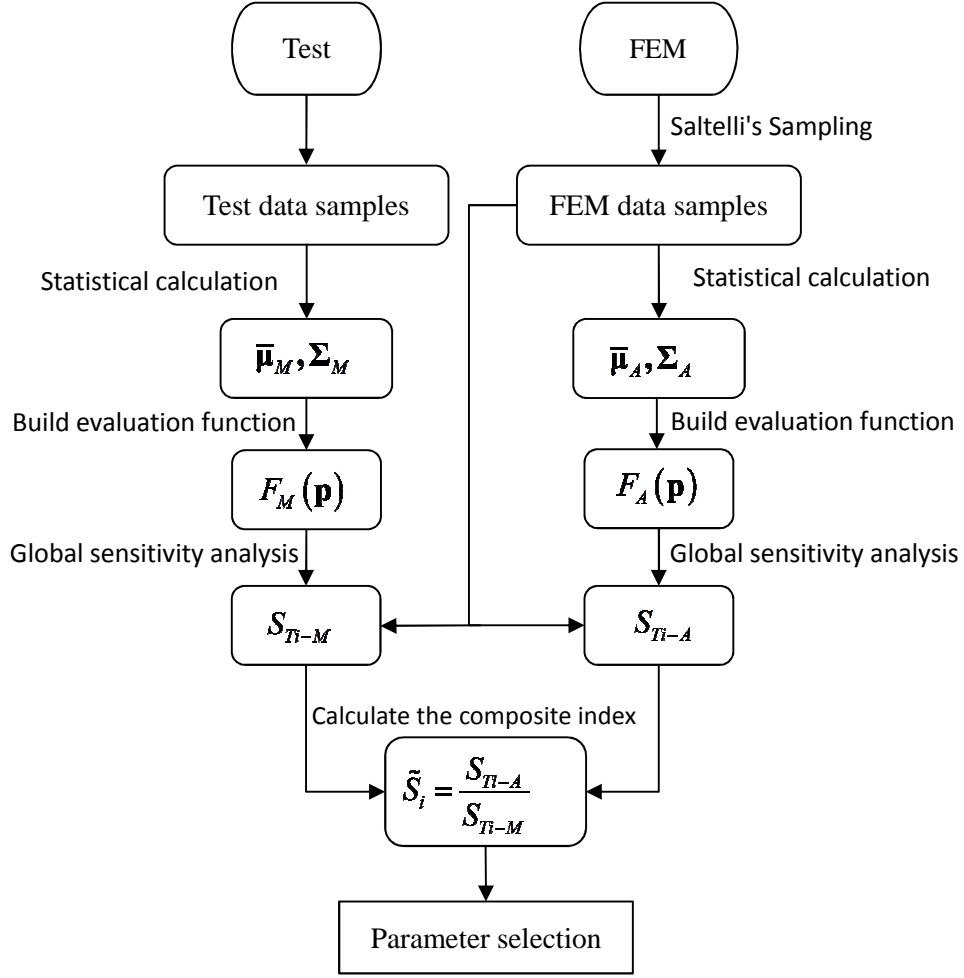


**Figure 1.** Flowchart of the method.

## 2.1 Building the evaluation function

Consider an analytical finite element model with input parameter vector  $\mathbf{p} = (p_1, p_2, \dots, p_n)^T$  and the output of modal frequencies  $\boldsymbol{\omega}_A = (\omega^1, \omega^2, \dots, \omega^k)_A^T$ , where  $n$  is the number of parameters to be selected and  $k$  is the number of output modal frequencies. The model can be described as a function,

$$\boldsymbol{\omega}_A = f_A(\mathbf{p}) \quad (1)$$

The model output is described here as the modal natural frequencies, but could include mode shapes, frequency response functions or any other model output.

The corresponding test data measurement can be described as a random vector for each of  $k$

natural frequencies  $(\boldsymbol{\omega}_M^i)^T = (\omega_1^i, \omega_2^i, \dots, \omega_m^i)_M$ ;  $i = 1, 2, \dots, k$  obtained typically from tests carried out on  $m$  nominally identical structures. To show no preference for any particular output, the samples from finite element analysis and test are scaled with the mean of the test data  $\mu_M^i = E[\boldsymbol{\omega}_M^i]$  such that,

$$\mathbf{y}_A^i = \frac{\boldsymbol{\omega}_A^i}{\mu_M^i} = \frac{f_A^i(\mathbf{p})}{\mu_M^i} \quad (2)$$

$$\mathbf{y}_M^i = \frac{\boldsymbol{\omega}_M^i}{\mu_M^i} \quad (3)$$

Then the normalized mean  $\bar{\boldsymbol{\mu}}_M$  and the covariance matrix  $\boldsymbol{\Sigma}_M$  may be determined as,

$$\begin{aligned} \bar{\boldsymbol{\mu}}_M &= \mathbf{I} = (1, 1, \dots, 1)_n^T \\ \boldsymbol{\Sigma}_M &= \mathbb{E} \left[ (\mathbf{y}_M - \mathbf{I})(\mathbf{y}_M - \mathbf{I})^T \right] \end{aligned} \quad (4)$$

Similarly, by sampling from a multivariate normal distribution of the modelling parameters, and in preparation for later requirement in Section 2.3, the mean  $\bar{\boldsymbol{\mu}}_A$  and the covariance matrix  $\boldsymbol{\Sigma}_A$  of the normalized finite element model output samples may be obtained by forward propagation.

Then, from (4) an evaluation function in the form of a log multivariate normal distribution PDF may be constructed as,

$$F_M(\mathbf{p}) = \log \text{PDF}_M(\mathbf{y}_A(\mathbf{p})) = \log \left( \frac{\exp \left( -\frac{1}{2} (\mathbf{y}_A(\mathbf{p}) - \mathbf{I})^T \boldsymbol{\Sigma}_M^{-1} (\mathbf{y}_A(\mathbf{p}) - \mathbf{I}) \right)}{\sqrt{(2\pi)^k |\boldsymbol{\Sigma}_M|}} \right) \quad (5)$$

The log form of multivariate normal distribution PDF gives a higher gradient when the sample is far from the mean value, as illustrated in Fig. 2. This can be helpful in preventing the sensitivity from becoming too small when the samples are far from the mean of the test data. The evaluation function (5) is based upon the mean and variance of the measured data, whereas  $\mathbf{y}_A(\mathbf{p})$  is an output of the model. It is therefore a mixture of the test and the model and represents an approximation to the unknown true log-density of the measured output. If

the PDF is sharply peaked, then  $F_M(\mathbf{p})$  is seen to be sensitive to a small change in the model output. Conversely, when the PDF is shallow  $F_M(\mathbf{p})$  will be insensitive. Clearly, the PDF will be sharply peaked when the variance of the output is low, and shallow when the variance is high. It is not possible to say whether or not  $F_M(\mathbf{p})$  is sensitive to a particular set of parameters without considering the effect of the chosen parameters on the output.

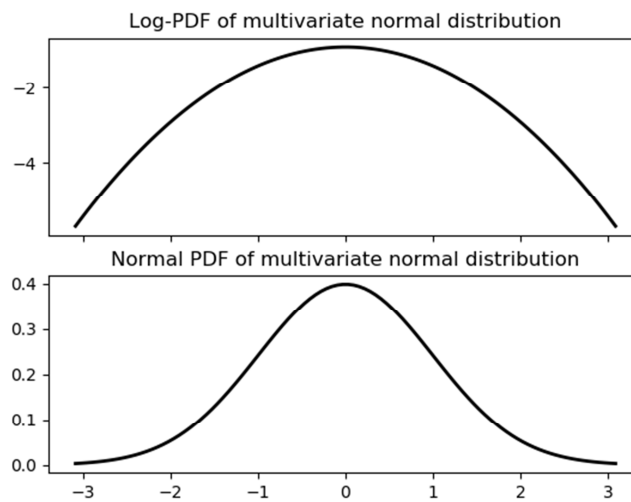


**Figure 2.** Log-PDF of multivariate normal distribution.

## 2.2 Global sensitivity analysis

There are many ways of calculating the global sensitivity indices including Fourier Amplitude Sensitivity Test (FAST) [22], the method of Morris [23], the Derivative-based Global Sensitivity Measure (DGSM) and Delta Moment-Independent Measure [25]. Here Sobol's sensitivity analysis method (originally developed by Sobol [26] then improved by Saltelli [27], [28]) is adopted for reasons of robustness and widespread usage. All these methods share the same concept of global sensitivity analysis, so any of them may be used in the research presented here. Below are some key steps to calculate the sensitivity indices with Sobol's method.

Given an evaluation model of the form  $Z = F_M(p_1, p_2, \dots, p_n)$ , with  $Z$  a scalar, the first

order effect by variance may be written as,

$$V_{p_i} = \mathbb{V}_{p_i} \left( \mathbb{E}_{p_{\sim i}} [Z | p_i] \right) \quad (6)$$

where  $\mathbb{V}(\bullet)$  and  $\mathbb{E}[\bullet]$  are the variance and expectation operators respectively,  $p_i$  is the  $i^{\text{th}}$  input and  $p_{\sim i}$  denotes the matrix of all inputs except  $p_i$ . Then the first-order Sobol sensitivity index may be determined by the expression,

$$S_i = \frac{\mathbb{V}_{p_i} \left( \mathbb{E}_{p_{\sim i}} [Z | p_i] \right)}{\mathbb{V}(Z)} \quad (7)$$

and the total effect index by,

$$S_{Ti} = \frac{\mathbb{E}_{p_{\sim i}} \left[ \mathbb{V}_{p_i} (Z | p_{\sim i}) \right]}{\mathbb{V}(Z)} = 1 - \frac{\mathbb{V}_{p_{\sim i}} \left( \mathbb{E}_{p_i} [Z | p_{\sim i}] \right)}{\mathbb{V}(Z)} \quad (8)$$

$S_{Ti}$  measures the first and all higher order effects of the input  $p_i$ . It can be seen that the theoretical calculation of these indices requires the theoretical probability distribution function which for practical reasons is usually determined by Monte Carlo simulation.

The key to Sobol's method is the decomposition of the evaluation function,

$$\begin{aligned} Z = F(p_1, p_2, \dots, p_n) = & F_0 + \sum_{i=1}^n F_i(p_i) + \sum_{1 \leq i < j \leq n} F_{ij}(p_i, p_j) \\ & + \dots + F_{1,2,\dots,n}(p_1, p_2, \dots, p_n) \end{aligned} \quad (9)$$

where  $F_0$  is a constant and the integral of each item  $F_{i_1, i_2, \dots, i_s}(p_{i_1}, p_{i_2}, \dots, p_{i_s})$  over any independent variable is zero,

$$\int F_{i_1, i_2, \dots, i_s}(p_{i_1}, p_{i_2}, \dots, p_{i_s}) dp_{i_j} = 0; \quad 1 \leq j \leq s \quad (10)$$

Using this decomposition, the mean value, the total and partial variances can be estimated with  $N$  samples [19],

$$\hat{\mathbb{E}}(Z) = \frac{1}{N} \sum_{m=1}^N F(\mathbf{p}_m) \quad (11)$$

$$\hat{V} = \hat{\mathbb{V}}(Z) = \frac{1}{N} \sum_{m=1}^N F^2(\mathbf{p}_m) - \left( \hat{\mathbb{E}}[Z] \right)^2 \quad (12)$$

$$\hat{V}_{p_i} \left( \mathbb{E}_{p_{-i}} [Z | p_i] \right) = \frac{1}{N} \sum_{\substack{m=1 \\ q \neq m}}^N F(\mathbf{p}_{(-i)m}, p_{im}) F(\mathbf{p}_{(-i)q}, p_{im}) - \left( \hat{\mathbb{E}}[Z] \right)^2 \quad (13)$$

In these equations,  $\mathbf{p}_m = (p_{1m}, p_{2m}, \dots, p_{nm})$  denotes the  $m$ -th sample and  $\mathbf{p}_{(-i)m}$  is given by excluding  $p_{im}$  such that,

$$\mathbf{p}_{(-i)m} = (p_{1m}, p_{2m}, \dots, p_{(i-1)m}, p_{(i+1)m}, \dots, p_{nm}) \quad (14)$$

The subscript  $q$  in Eq. (13) indicates that two different samples,  $m$  and  $q$ , are used. The same equation may be used to calculate the first order sensitivity indices, and a similar formula leads to an expression for the total sensitivity index,

$$\hat{V}_{p_{-i}} = \hat{V}_{p_{-i}} \left( \mathbb{E}_{p_i} [Z | p_{-i}] \right) = \frac{1}{N} \sum_{\substack{m=1 \\ q \neq m}}^N F(\mathbf{p}_{(-i)m}, p_{im}) F(\mathbf{p}_{(-i)m}, p_{iq}) - \left( \hat{\mathbb{E}}[Z] \right)^2 \quad (15)$$

$$\hat{S}_{Ti} = 1 - \hat{V}_{p_{-i}} / \hat{V} \quad (16)$$

When using these formulas, one should pay attention to the subscripts in Eq. (13) and Eq. (15), which are different. This arises because of the different meanings of first-order and total sensitivity indices. For each sample term in Eq. (13), all variables except the studied parameter are changed, which has the effect of removing its contribution alone. But in Eq. (15), only the studied parameter is changed, and Eq. (16) may then be used to calculate its total effect.

In the present research, the parameters show an obviously high order effect brought by the interaction of parameters in the finite element analysis. Therefore, the total sensitivity indices will be mainly used. Fortunately, there is a powerful open source Python library called SALib [29] which provides a convenient way to access most popular GSA methods [26][27][28] and is validated to be effective and efficient. The sampling procedure and the sensitivity evaluation were carried out using the functions available in this toolbox.

### 2.3 A composite index for parameter selection.

This section begins with a baseline (or reference) function defined in the same way as the evaluation function, but with finite element data only and given by,

$$F_A(\mathbf{p}) = \log \left( \frac{\exp \left( -\frac{1}{2} (\mathbf{y}_A(\mathbf{p}) - \bar{\boldsymbol{\mu}}_A)^T \boldsymbol{\Sigma}_A^{-1} (\mathbf{y}_A(\mathbf{p}) - \bar{\boldsymbol{\mu}}_A) \right)}{\sqrt{(2\pi)^k |\boldsymbol{\Sigma}_A|}} \right) \quad (17)$$

where the mean  $\bar{\boldsymbol{\mu}}_A$  and the covariance matrix  $\boldsymbol{\Sigma}_A$  are determined, as explained in Section 2.1.

Normally, global-sensitivity sampling is based on Latin-Hypercube or a similar unbiased uniform distribution. This means the baseline function (17) will give an evaluation of the sensitivity of the finite element model parameters in the same way as conventional global-sensitivity-based parameter selection methods. Then, to eliminate unwanted model effects a new composite index may be created by dividing the baseline total sensitivity index by the same index from the evaluation function,

$$\tilde{S}_i = \frac{S_{Ti-A}}{S_{Ti-M}} = \frac{\mathbb{E}_{p_{\sim i}} \left[ \frac{\nabla_{p_i} (F_A(\mathbf{p}) | p_{\sim i})}{\nabla (F_A(\mathbf{p}))} \right]}{\mathbb{E}_{p_{\sim i}} \left[ \frac{\nabla_{p_i} (F_M(\mathbf{p}) | p_{\sim i})}{\nabla (F_M(\mathbf{p}))} \right]} \quad (18)$$

Here,  $S_{Ti-A}$  defines the contribution of selected parameters to the total sensitivity by using the baseline function. Similarly,  $S_{Ti-M}$  is determined from the evaluation function (5) to give the contributions of the same parameters. If the statistics of the  $i^{\text{th}}$  parameter are accurately represented in the model then  $S_{Ti-A}$  and  $S_{Ti-M}$  should be the same and the composite index  $\tilde{S}_i$  should be equal to unity. Parameters with erroneously modelled statistics will be marked by the deviation of  $\tilde{S}_i$  from unity.

### 3 Numerical case study

#### 3.1 Pin-joined truss

As shown in Figure 3, a pin-jointed truss structure of overall dimensions  $5\text{m} \times 1\text{m}$  and composed of 21 bar elements of cross-sectional area  $0.03 \text{ m}^2$ , will be used as a simulated numerical case study. Each bar element of density  $2700 \text{ kg/m}^3$  has a nominal elastic modulus  $7.0 \times 10^{10} \text{ Pa}$ , which is randomised with a multivariate normal distribution and considered as

a candidate for updating. The mean and standard deviation,  $\mu_i = 7.0 \times 10^{10} \text{ Pa}$  and  $\sigma_i = 0.05 \times \mu_i = 0.05 \times 7.0 \times 10^{10} \text{ Pa}$ ,  $i = 1, 2, \dots, 21$ , respectively, are applied throughout. Therefore, the whole structure is an uncertain system with 21 randomized parameters. Then, in what follows, the mean and standard deviation values of the elastic moduli of the chosen parameters are changed to simulate highly erroneous parameters in the structure. Modal frequency data are used as the nominal measured output and using the parameter selection method presented in Section 2, the parameters that contribute most to the uncertainty of the structure will become apparent. Since the structure and target parameter list are the same as those described by Silva et al. [21], it is only necessary here to discuss the selection of parameters.

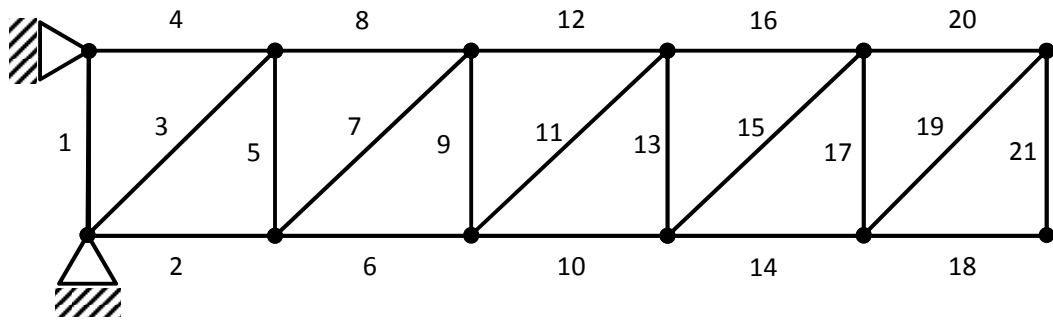


**Figure 3.** Pin-jointed truss.

### 3.2 Independent parameters case

The first case is when the parameters to be selected are independent of each other. Then, using numbering of elements as in Figure 3, the diagonal bars listed as  $\{3, 7, 11, 15, 19\}$  are chosen as target parameters. The mean values of these parameters are set to  $\tilde{\mu}_i = 6.3 \times 10^{10} \text{ Pa}$  and set the standard deviations to  $\tilde{\sigma}_i = 0.17 \times \mu_i = 0.25 \times 7.0 \times 10^{10} \text{ Pa}$ ,  $i = 3, 7, 11, 15, 19$ . Modal frequency samples are then generated with these new parameters and used as the nominal test data for parameter selection.

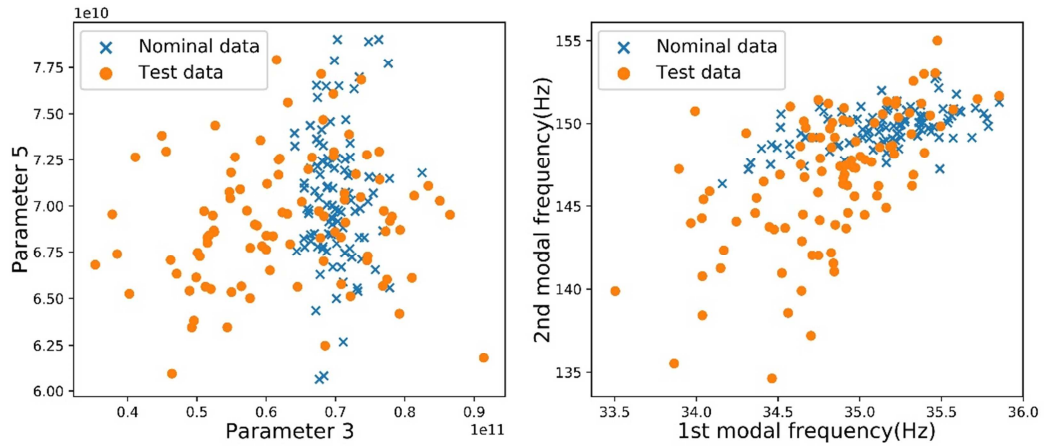
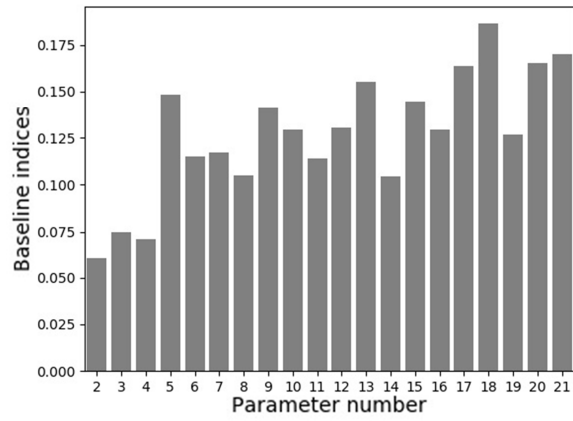


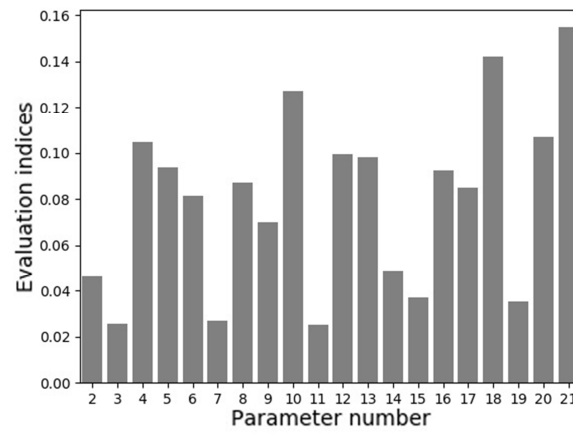
**Figure 4.** The change in parameters(left) and modal frequencies(right).

It can be seen in Figure 4 that test parameter  $p_3$ , which is one of the listed parameters has an increased deviation, whereas the standard deviation of  $p_5$  remains unchanged. The change in modal frequencies associated with the parameters is also shown in the figure.

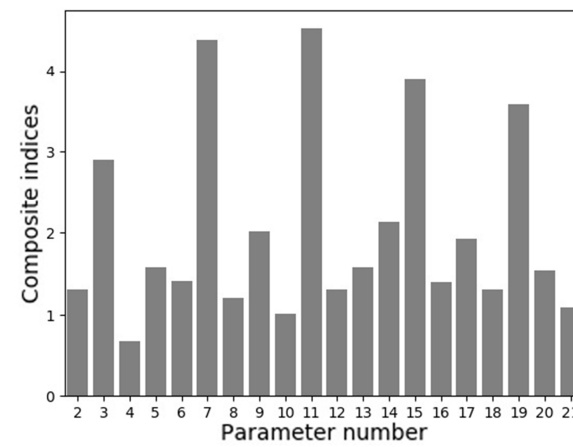
The extension of Sobol's method by Saltelli et al. [27], [28] reduces the errors in the sensitivity index calculations, and was used for the sampling of the finite element data. Here, the interval of all parameters was set to  $\pm 30\%$  of the initial mean values, i.e.  $[0.7-1.3] \times 7.0 \times 10^{10}$  Pa for every candidate parameter and the composite sensitivity indices determined using the procedure explained previously.



(a)  $S_{Ti-A}$



(b)  $S_{Ti-M}$



(c)  $\tilde{S}_i$

**Figure 5.** (a) Baseline, (b) Evaluation, (c) Composite indices

It is seen in Figure 5 that it is not possible to distinguish the erroneous parameters from the sensitivity indices of the baseline function. The evaluation function indices, however, show the parameters with correctly modelled statistics to be much greater than the others and similar in value to the baseline-function indices. All the composite indices for the correctly modelled parameters are close to unity, as expected, while the parameters with erroneous statistics {3, 7, 11, 15, 19} have much higher composite indices. Thus, all the expected parameters would be selected for updating.

### 3.3 Correlated parameters case

In many cases, the random structural parameters may not be independent of each other. Similar to the independent case, the test data were generated with a random parameter sample, but this time the parameters in the target list were deliberately correlated. The target list for selection was the same as before, i.e. {3,7,11,15,19}. The mean values of the parameters were set as in the previous case to  $\tilde{\mu}_i = 6.3 \times 10^{10} \text{ Pa}$ ,  $i = 3, 7, 11, 15, 19$ . Parameter pairs {3,7} and {15,19} were correlated as shown in the covariance matrix,

$$\begin{aligned} \text{diag}(\boldsymbol{\Sigma}_M) &= \begin{cases} (0.17 \times 7.0 \times 10^{10} \text{ Pa})^2, & i = 3, 7, 11, 15, 19 \\ (0.05 \times 7.0 \times 10^{10} \text{ Pa})^2, & i \neq 3, 7, 11, 15, 19 \end{cases} \\ \text{non-diag}(\boldsymbol{\Sigma}_M) &= \begin{cases} (0.17 \times 7.0 \times 10^{10})^2 \text{ Pa}^2, & i = 3, 7 \\ -(0.13 \times 7.0 \times 10^{10})^2 \text{ Pa}^2, & i = 15, 19 \\ 0 \text{ Pa}^2, & i \neq 3, 7, 15, 19 \end{cases} \end{aligned}$$

Parameter samples generated from this distribution are shown in the scatter diagrams and histograms of Figure 6. Parameter pair {3,7} is seen to have a complete positive linear correlation whereas parameter pair {15,19} have an incomplete negative linear correlation.

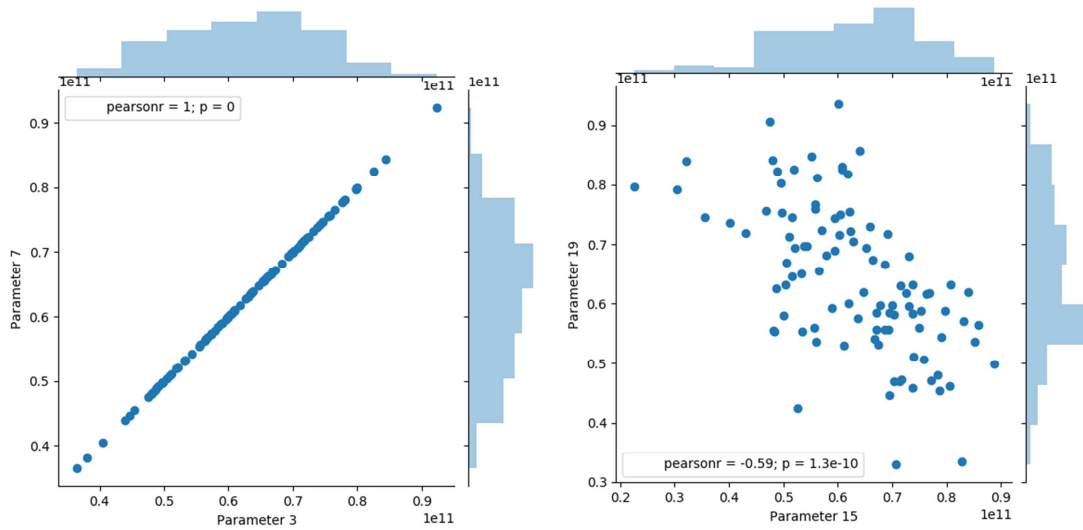


**Figure 6.** Generated correlated parameter samples.

Here again the presented composite index is used for parameter selection, and the sample interval for global sensitivity analysis remains as before,  $[0.7-1.3] \times 7.0 \times 10^{10}$  Pa.

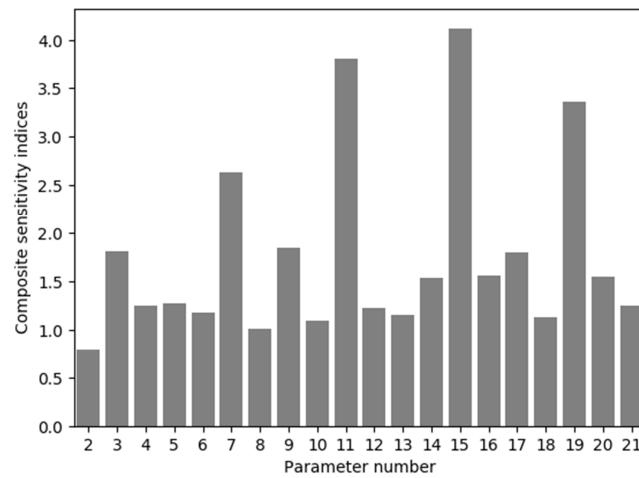


**Figure 7.** Composite sensitivity indices calculation result for correlated parameters.

From the result shown in Figure 7, the list  $\{3,7,11,15,19\}$  can still be distinguished, but the value for parameter 3 is lower than other targeted parameters. This is caused by the correlation of parameters. As shown in Figure 6, parameters  $p_3$  and  $p_7$  have a very strong correlation, which makes them affected more than parameter pair  $(p_{15}, p_{19})$ . However, parameter  $p_9$  may be mistakenly selected, which is not exactly what we want, but for most

model updating problems, selecting a limited extra number of parameters than needed will not have much effect on the updating result. Thus, correlated parameters may also be selected by the method presented in this paper.

## 4 Experimental case study

### 4.1 Test structure and modal test results

In order to validate the methodology proposed in this paper, the physical aluminium frame structure shown in Figure 8, with mass-position uncertainty, was investigated. It was built with beams and movable mass blocks of 2.03 kg. The frame was fixed to a rigid base with four bolts and the mass blocks were machined with a ridge that formed a line of contact with the beams at the level of the centre of mass. The vertical positions of the masses could be adjusted to represent structural variability while the horizontal (axis  $x$ ) position remained unchanged. The mass centres of the two blocks were always on the vertical centre lines of the short vertical beams.

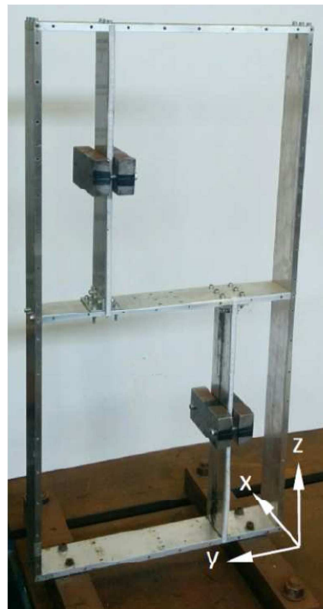


**Figure 8.** Frame structure with mass-position uncertainty.

The natural frequencies of the frame were the measured outputs. The problem of

randomness among nominally identical structure was then simulated by moving the two masses to different positions denoted by  $p_1$  and  $p_2$ . The distance from the bottom horizontal beam to the lower mass was  $p_1$  and that from the middle horizontal beam to the upper mass was  $p_2$ . The overall height of frame was 80cm and the maximum feasible regions of variability of  $p_1$  and  $p_2$  was from 10 cm to 30 cm. In total 100 positional pairs  $(p_1, p_2)$  were designed to follow a bivariate normal distribution with mean  $\bar{\mu}_M = (20, 20)^T$  and covariance matrix  $\Sigma_M = \begin{bmatrix} 9.97 & 5.63 \\ 5.63 & 9.97 \end{bmatrix}$ , being the statistics determined from the 100 observations, as shown in Figure 9, and not the generating statistics. The two parameters were found to be correlated with a Pearson correlation coefficient of 0.59.

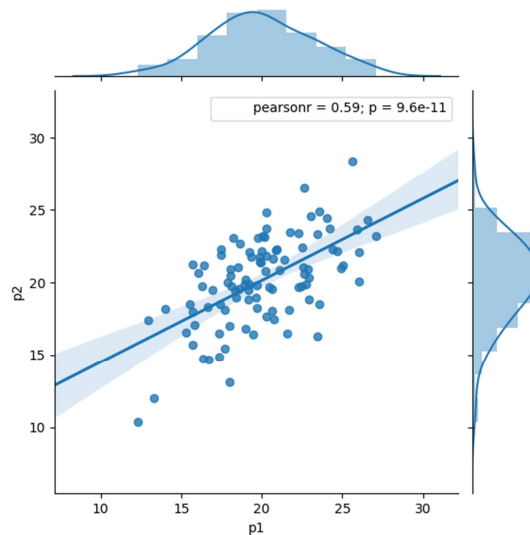


**Figure 9.** Generated mass position samples.

Modal tests were carried out with the two masses arranged according to the distribution outlined. Roving hammer excitation was applied in two perpendicular directions with accelerometers placed accordingly and the first twelve modal natural frequencies were extracted using the Siemens PLM / LMS Testlab system and the PolyMax algorithm. The sampling frequency was 512Hz, slightly lower than the Nyquist frequency usually require to accurately determine the 12<sup>th</sup> mode at around 280Hz, but apparently without problems of aliasing. Figure 10 shows probability density functions generated from the test results for

each of the 12 natural frequencies. The legend in the middle of the figure shows the order of the modes.

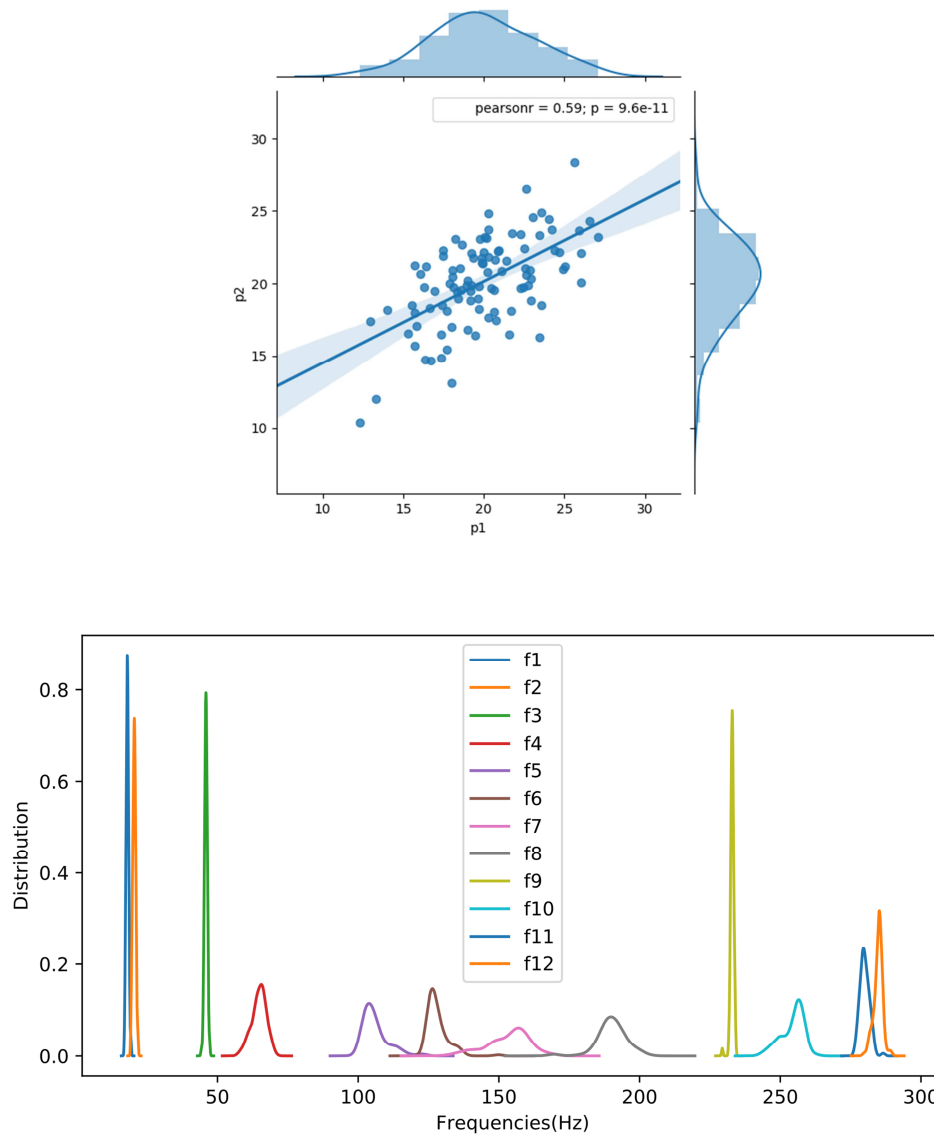


**Figure 10.** Distributions of the test data.

## 4.2 The finite element and Kriging surrogate models

A finite element model consisting of beam elements was used to represent the physical structure. The two vertical interior beams were each modelled using 40 beam elements thereby allowing the placement of the masses to be chosen from 39 nodal points. This causes a problem because it is generally not possible to reproduce the experimental mass-position distributions in the FE model without placing the masses at intermediate positions between the nodes. A Kriging surrogate model was constructed to overcome this problem.

Kriging has found widespread application in structural dynamic research [30-34] and in present example was built using input and output samples generated from the finite element model. The five parameters listed in Table 1 were chosen as input. These include not only the positions of the two masses but also the bolt stiffnesses,  $k_b$ , that connect the bottom of the frame to the rigid base and shear moduli,  $G_b$  and  $G_v$ , for the horizontal base beam and the two interior vertical beams. Stiffness  $k_b$  was considered to be potentially nonlinear, since similar boundary-condition stiffnesses are common sources of error in many model updating exercises.  $G_b$  and  $G_v$ , are the beam stiffness parameters in key areas of the structure most affected by the bending and twisting modes of the structure. It is seen from the table that mean values of the mass positions are exactly the same as in the test and the standard deviations are close to test values, although these might not be exactly reproduced in Latin hypercube sampling from a uniform distribution by Sobol's method. The mean of the base restriction stiffness was determined by an informed guess and the shear moduli ( $p_4, p_5$ ) are given by standard values for aluminium.

**Table 1.** Parameter descriptions and initial statistics

Parameter	Mean $\tilde{\mu}_i$	STD $\tilde{\sigma}_i = 0.173 \times \tilde{\mu}_i$	Description
$p_1$	20 cm	3.464 cm	Position of upper mass block
$p_2$	20 cm	3.464 cm	Position of lower mass block
$p_3 = k_b$	$2 \times 10^7$ kg/m	$0.346 \times 10^7$ kg/m	Base restriction stiffness
$p_4 = G_b$	$2.594 \times 10^{10}$ Pa	$0.449 \times 10^{10}$ Pa	Shear modulus - base beam
$p_4 = G_v$	$2.594 \times 10^{10}$ Pa	$0.449 \times 10^{10}$ Pa	Shear modulus - interior vertical beams

The Kriging model consisting of a hyperspace of five dimensions with  $8^5 = 32,768$  training points for each of the 12 natural frequencies was found to reproduce the finite element results with very good accuracy. Figure 11 is generated by the trained Kriging model, in which the x-

and y-axes present the parameters  $p_1$  and  $p_2$  respectively, and the z-axis is the 6<sup>th</sup> modal frequency. The black dots on the figure are random samples (different from the training points) generated from the finite element model. It can be seen the model fits them well, which means the Kriging model is capable of representing the behaviour of the finite element model.

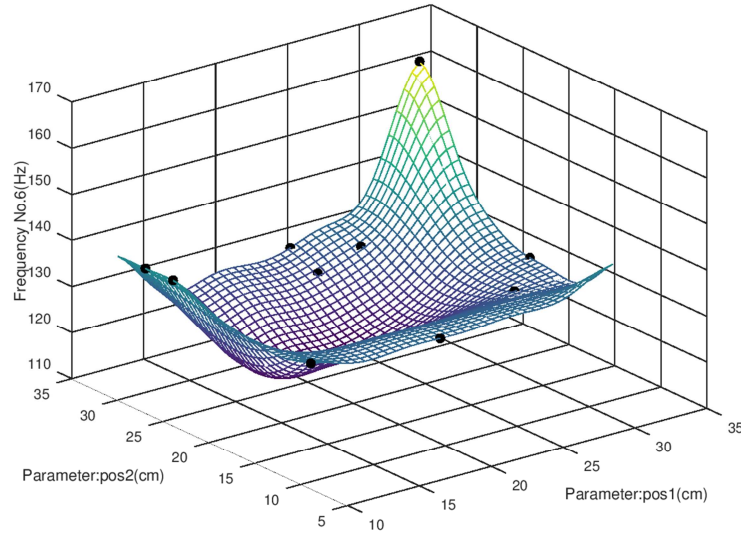
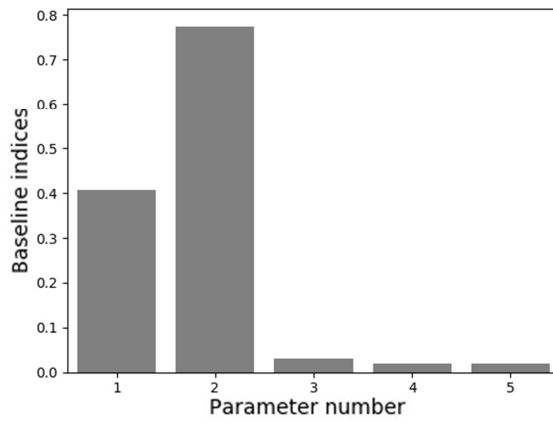


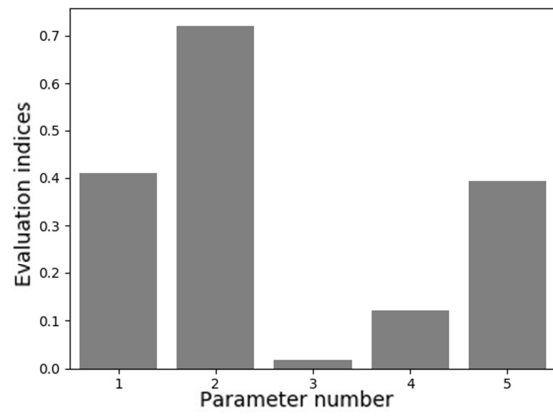
**Figure 11.** The trained Kriging surrogate model.

### 4.3 Parameter selection

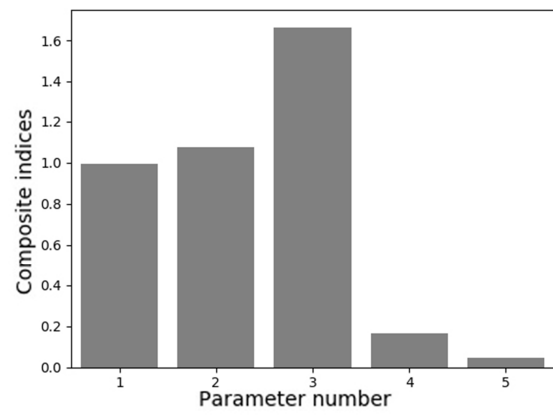
Figure 12 shows the parameter selection result obtained by the proposed method in terms of the composite sensitivity index. As can be seen, parameters  $p_1$  and  $p_2$  which are the position of the mass blocks, have similar index values for  $S_{Ti-A}$  and  $S_{Ti-M}$ , and for the composite index have values very close to unity. This is to be expected because the Kriging model was based on the exact mean of test and the standard deviation is close to that obtained from measurement. This result confirms that the statistics of the mass positions used in the model are a close match to the test and therefore  $p_1$  and  $p_2$  are not in need of updating. We know from engineering judgement that the beam shear moduli  $p_4$  and  $p_5$  are likely to be deterministic, so although some updating may be necessary, deterministic updating should suffice. The base restriction stiffness  $p_3$  is more complicated and may be nonlinear.



(a)  $S_{Ti-A}$



(b)  $S_{Ti-M}$



(c)  $\tilde{S}_i$

**Figure 12.** (a) Baseline, (b) Evaluation, (c) Composite indices

Another interesting result of the parameter selection is the second order global sensitivity indices result shown in Figure 13. The x-axis and y-axis are the indices of the parameters and the colour denotes the sensitivity indices. It is seen that there is a very high value between parameters  $p_1$  and  $p_2$ , which in fact are correlated. So the presented evaluation function can also be used as a correlation evaluation tool for the uncertain parameters in the structure.

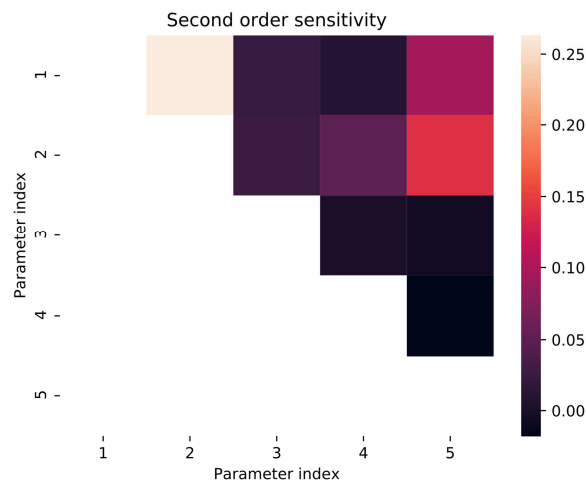


**Figure 13.** Second order global sensitivity for the experimental case.

## 5 Conclusions

In this paper, a parameter selection method for stochastic model updating is presented. The method is based global sensitivity analysis using a new evaluation function, assumed to be a close approximation to the PDF of the measured data. This leads to a composite sensitivity index, by dividing indices from a baseline function by those from the evaluation function. This process allows the discrimination of parameters with correctly modelled statistics from the erroneous ones. Two simulation cases studies are presented with parameter selection carried out on a pin-jointed truss structure. In the first study, the uncertain parameters are taken to be independent and in the second the parameters are correlated. All stiffness parameters in the structure are randomized with chosen mean values and standard deviations, but only a subset of these are erroneous. Excellent results were obtained in both cases.

The methodology is validated experimentally on a frame structure with masses in uncertain positions. The presented method confirm that the statistics of the mass positions are correctly modeled and not in need of updating. Furthermore, the second-order global sensitivity of the evaluation function identified the correlation of the two position parameters.

### **Acknowledgement**

The research was supported by the National Science Foundation of China (NSFC) under Grant No. 11372084 and the China Scholarship Council (CSC). It was carried out during a visit to the University of Liverpool by Mr Zhaoxu Yuan and was supervised by Professor John E Mottershead.

### **References**

- [1] J.E. Mottershead and M.I. Friswell, Model updating in structural dynamics: a survey, *Journal of Sound and Vibration* 167.2 (1993): 347-375.
- [2] M.I. Friswell and J.E. Mottershead, *Finite element model updating in structural dynamics*. Kluwer Academic Publishers, Dordrecht, 1995.
- [3] M.I. Friswell, J.E Mottershead, H. Ahmadian, Combining subset selection and parameter constraints in model updating, *Journal of Vibration and Acoustics*, 120 (1998) 854-859.
- [4] H. Ahmadian, G. Gladwell, F. Ismail, Parameter selection strategies in finite element model updating, *Journal of Vibration and Acoustics*, 119 (1997) 37-45.
- [5] J.E. Mottershead, C. Mares, M.I. Friswell, S. James, Selection And Updating Of Parameters for an Aluminium Space-Frame Model, *Mechanical Systems and Signal Processing*, 14 (2000) 923-944.
- [6] N. Abu Husain, H. Haddad Khodaparast, H. Ouyang, Parameter selection and stochastic model updating using perturbation methods with parameter weighting matrix assignment, *Mechanical Systems and Signal Processing*, 32 (2012) 135-152.
- [7] A.J. Millar, *Subset Selection in Regression*, Monographs on Statistics and Applied Probability, Chapman and Hall, 40 (1990).
- [8] G. Lallement and J. Piranda, Localization Methods for Parameter Updating of Finite Element Models in Elastodynamics, 8th International Modal Analysis Conference, Orlando, Florida, (1990) 579-585.
- [9] T.F. Chan and P.C. Hansen, Some Applications of the Rank Revealing QR Factorization, *SIAM Journal on Scientific and Statistical Computing*, 13 (1992) 727-741.

- [10] G.-H. Kim and Y.-S. Park, An improved updating parameter selection method and finite element model update using multiobjective optimisation technique, *Mechanical Systems and Signal Processing*, 18 (2004) 59-78.
- [11] G.-H. Kim and Y.-S. Park, An automated parameter selection procedure for finite-element model updating and its applications, *Journal of Sound and Vibration*, 309 (2008) 778-793.
- [12] L. Mthembu, T. Marwala, M.I. Friswell and S. Adhikari, Model selection in finite element model updating using the Bayesian evidence statistic, *Mechanical Systems and Signal Processing*, 25 (2011) 2399-2412.
- [13] S.-E. Fang and R. Perera, Damage identification by response surface based model updating using D-optimal design, *Mechanical Systems and Signal Processing*, 25 (2011) 717-733.
- [14] S.-E. Fang, W.-X. Ren and R. Perera, A stochastic model updating method for parameter variability quantification based on response surface models and Monte Carlo simulation, *Mechanical Systems and Signal Processing*, 33 (2012) 83-96.
- [15] A. Saltelli, D. Gatelli, F. Campolongo, J. Cariboni, M. Ratto, M. Saisana, and T. Andres. *Global Sensitivity Analysis: The Primer*. John Wiley & Sons, 2008.
- [16] A. Saltelli, K. Chan, and E.M. Scott (Eds), *Sensitivity Analysis*. Wiley Series in Probability and Statistics, Wiley, 2000.
- [17] G. Boscato, S. Russo, R. Ceravolo, L.Z. Fragonara, Global Sensitivity-Based Model Updating for Heritage Structures, *Computer-Aided Civil and Infrastructure Engineering*, 30 (2015) 620-635.
- [18] H.-P. Wan, W.-X. Ren, Parameter Selection in Finite-Element-Model Updating by Global Sensitivity Analysis Using Gaussian Process Metamodel, *Journal of Structural Engineering*, 141 (2015) 04014164.
- [19] B. Sudret, Global sensitivity analysis using polynomial chaos expansions, *Reliability Engineering & System Safety*, 93 (2008) 964-979.
- [20] B. Moaveni, J.P. Conte, and F.M. Hemez, Uncertainty and sensitivity analysis of damage identification results obtained using finite element model updating, *Computer Aided Civil and Infrastructure Engineering*, 24.5 (2009): 320-334.
- [21] T.A.N. Silva, N.M.M. Maia, M. Link, J.E. Mottershead, Parameter selection and covariance updating, *Mechanical Systems and Signal Processing*, 70-71 (2016) 269-283.
- [22] R.I. Cukier, CM Fortuin, KE Shuler, AG Petschek, JH Schaibly, Study of the sensitivity of coupled reaction systems to uncertainties in rate coefficients. I Theory, *Journal of Chemical Physics*, 59.8 (1973): 3873-3878.
- [23] M.D. Morris, Factorial sampling plans for preliminary computational experiments, *Technometrics*, 33.2 (1991): 161-174.
- [24] S. Kucherenko, Derivative based global sensitivity measures and their link with global sensitivity indices, *Mathematics and Computers in Simulation*, 79.10 (2009): 3009-3017.

- [25] E. Borgonovo, A new uncertainty importance measure, *Reliability Engineering & System Safety*, 92.6 (2007): 771-784.
- [26] I.M. Sobol, Global sensitivity indices for nonlinear mathematical models and their Monte Carlo estimates, *Mathematics and computers in simulation*, 55.1 (2001): 271-280.
- [27] A. Saltelli, Making best use of model evaluations to compute sensitivity indices, *Computer Physics Communications*, 145.2 (2002): 280-297.
- [28] A. Saltelli, P. Annoni, I. Azzini, F. Campolongo, M. Ratto, S. Tarantola, Variance based sensitivity analysis of model output. Design and estimator for the total sensitivity index, *Computer Physics Communications*, 181.2 (2010): 259-270.
- [29] J. Herman and W. Usher. SALib: an open-source Python library for sensitivity analysis, *The Journal of Open Source Software*, 2.9 (2017).
- [30] F.A. DiazDelaO, and S. Adhikari, Gaussian process emulators for the stochastic finite element method, *International Journal for Numerical Methods in Engineering*, 87.6 (2011): 521-540.
- [31] T.E. Fricker, J.E. Oakley, N. D. Sims, K. Worden, Probabilistic uncertainty analysis of an FRF of a structure using a Gaussian process emulator. *Mechanical Systems and Signal Processing*, 25.8 (2011): 2962-2975.
- [32] G. Mehdi, K. J. Badcock, and M. A. Woodgate, Accelerating the numerical generation of aerodynamic models for flight simulation. *Journal of Aircraft*, 46.3 (2009): 972-980.
- [33] H.-P. Wan, W.-X. Ren, A residual-based Gaussian process model framework for finite element model updating, *Computers and Structures*, 156 (2015) 149–159.
- [34] H.-P. Wan, Z. Mao, M.D. Todd, W.-X. Ren, Analytical uncertainty quantification for modal frequencies with structural parameter uncertainty using a Gaussian process metamodel, *Engineering Structures*, 75 (2014) 577–589.